J. Mater. Environ. Sci. 6 (10) (2015) 2895-2905 *Sadik et al.*
ISSN : 2028-2508
CODEN: JMESCN

Sulfate removal from wastewater by mixed oxide-LDH: Equilibrium, kinetic and thermodynamic studies

R. Sadik*, R. Lahkale, N. Hssaine, W. ElHatimi, M. Diouri and E. Sabbar*
Laboratory of Physic and Chemistry of Materials (LPCM). Department of Chemistry, University Chouaîb Doukkali, El Jadida, MOROCCO.

Received 19 Sept 2014, Revised 26 Sept 2015, Accepted 26 Sept 2015
** Corresponding authors: R. SADIK: sadik084@yahoo.fr and Prof. E. SABBAR: esabbar@yahoo.fr*

Abstract
The removal of sulfate from effluent is carried out by adsorption using a mixed oxide of magnesium and aluminum obtained after calcination of a layered double hydroxide. This work requires the control and optimization of various parameters such as the effect of contact time, pH, adsorbent dose and sulfate initial concentration. The removal of sulfate from effluent is a rapid process. In fact, in the ambient temperature (25°C), the adsorption equilibrium is reached after 60 min. The adsorption capacity for the uptake of sulfate from effluent at 25˚C is 840mg/g. It is found that the adsorption kinetics is best described by the pseudo-second order model. Adsorption isotherms of sulfate are well fitted by Freundlich isotherm equation. The effect of temperature on the adsorption process of sulfate is also studied and the thermodynamic parameters are determined. The use of the mixed oxide is very interesting as an adsorbent. It allows the treatment of waste liquid and the regeneration of a LDH phase which can be used as precursor.

Keywords: Effluent; Sulfate; Adsorption; Thermodynamic, Mixed oxide-LDH;

1. .Introduction
The sulfate ion occurs naturally in most water supplies. It gets reduced biologically under anaerobic conditions to sulfide, which in turn combines with hydrogen to form hydrogen sulfide (H_2S) that causes concern due to color and pungent odor. The sources of metals in wastewater are mainly discharges from residential dwellings, ground water infiltration, mining drains, and commercial and industrial discharges.
Acidic sulfate wastewater, from electroplating, steel pickling, mining, nonferrous smelting and other related materials or substances, has become one main source of industrial and environmental pollution [1]. Several methods have been employed to treat sulfate-containing wastewater, including chemical precipitation [2], crystallization [3], ion exchange, [4] biological treatment [1], electro-dialysis [5], nano-filtration [6], reverse osmosis [7] and adsorption. Among them, adsorption is commonly considered to be the most attractive and mostly-used technique due to its efficacy and low cost [8, 9]. Activated carbon [10], hydrous iron oxide [11], γ-Al_2O_3 [12], chitin [13], etc, are used as adsorbents. However, the used materials still suffer from the low adsorption capacity and high-price for the sulfate wastewater treatment. Great interest has been directed toward the development of new types of adsorbents.

Then, it is very interesting to find other cheaper substituents such as layered double hydroxides(LDH). The layered double hydroxides (LDH) or hydrotalcite like compounds can be described by the general formula $[M^{2+}_{1-x}M^{3+}_{x}(OH)_2]^{x+}[X^{m-}_{x/m}, nH_2O]$ where M^{2+} is a cation of divalent metal , M^{3+} is cation of trivalent metal and X^{m-} represents an anion intercalated [14-17].The calcination of these LDH gives mixed oxides which are non-stoechiometric intermediate [18] and by rehydration provides their counterparts with different intercalated anions, called memory effect [19]. In this work, the adsorption of sulfate from effluent is performed by calcined hydrotalcite.

Various parameters are analyzed such as the effect of contact time, pH, adsorbent mass, initial sulfate concentration and temperature. At the end, we propose the retention mechanism of sulfates by our adsorbent.

2. Materials and methods

2.1 Material

2.1.1 Synthesis of the adsorbent

The preparation of the precursor is carried out under the method of cooprecipitation described by Reichle [20]. ($MgCl_2$, $6H_2O$) and ($AlCl_3$, $6H_2O$) are dissolved in distilled water with a molar ratio (Mg/Al = 3). The pH of the reaction mixture is maintained constant at 10.0 by adding a mixture of NaOH and Na_2CO_3 ([NaOH]/[Na_2CO_3] = 4). The gel is stirred at room temperature for 48h. The clay obtained is washed by centrifugation with distilled water and dried at 60°C for 48 h. The chemical formula of the clay prepared is $Mg_3Al(OH)_8(CO_3)_{0.5}$,$3.1H_2O$ (noted HT).The adsorbent used in this study is obtained by calcination of HT at 500°C during 5 h. The formula of this mixed oxide is $Mg_{2.95}AlO_{4.45}$ (noted HT500)

2.1.2. Effluent sample

The effluent sample has been collected and analysed by ICP:

Table.1. parameter effluent sample

ions	Concentration
SO_4^{2-} (mg/l)	4800
F^- (mg/L)	280-300
HPO_4^{2-} (mg/L)	280-300
pH	< 2

2.2 Analysis and characterization

All chemical reagents are of grade quality obtained from commercial sources and used without further purification. Chemical compositions of metals are determined by ICP (Induced coupled plasma (ICP) measurements) Emission Spectrophotometer. IR spectra are recorded in the range of 4000–400 cm^{-1} by FT-IR-8400S SHIMADZU spectrometer using KBr pellets (2%). The anionic clay is characterized by X-ray diffraction using 2 -D-diffractometer of Bruker-AXS PHASER using copper $K_{\alpha1}$ radiation (1.54056 Å) and $K_{\alpha2}$ (1.54439 Å). The dosage (nephelemetry method) is carried out by spectrophotometry (λ = 650nm) using a spectrophotometer type RAYLEIGH-Vis Spectrophotometer 7220G.

The-equilibrium sulfate concentration is measured as follows:

-Acidification by HCl (1M) the sulfate effluent SO_4^{2-} concentration in the solution

- Complexity of SO_4^{2-} present in effluent with polyvinyl pyrrolidone (PVP) solution (20 to 25%),

-The residual SO_4^{2-} concentration in the solution was determined by spectrophotometrically at 650 nm.

2.3 Batch Adsorption Studies

These experiments are performed by contacting 20 mg of HT500 with 50 ml of SO_4 effluent at desired contact time, pH, adsorbent mass, initial SO_4 concentration and temperature.

Once the equilibrium time is reached, the adsorbent is recovered by centrifugation. The amount of SO_4 retained per unit mass of solid at equilibrium is calculated by:

$$q_e = (C_0 - C_e)V/m \qquad (1)$$

Where q_e (mg/g) is the amount of SO_4 adsorbed per gram of adsorbent; m (g) is the mass of the adsorbent, and C_0 and C_e (mg/L) are the SO_4 concentrations respectively at t = 0 and at equilibrium time.

The SO_4 removal efficiency or SO_4 uptake (%) is calculated by:

$$(\%SO_4) = 100\ (C_0 - C_e)/C_0 \qquad (2)$$

3. Results and discussion

3.1. Characterization

3.1.1 X-ray diffraction

The typical XRD pattern (Figure 1) shows a lamellar structure of LDH material. The XRD patterns are indexed in the R-3m space group, where *c* is the lattice parameter corresponding to three times the interlayer distances ($c=3d_{003}$).The peak (110) indicates the intermetallic distance used to calculate *a* (lattice parameter ($a=2d_{110}$)).

The values of the parameters *c* and *a* are respectively 23.13 and 3.02Ǎ. These values are similar to those reported in literature [21-22].

The characterization of the HT500 performed byX-ray diffraction (Figure 2) shows the production of mixed oxide. Indeed, the disappearance of the characteristic pic of the HT is observed. That is to say, the structure is destroyed due to dehydroxylation of the sheet with the departure of water molecules and anions CO_3^{2-}. Obtaining the mixed oxide is confirmed by the non presence of a characteristic peak of simple oxides.

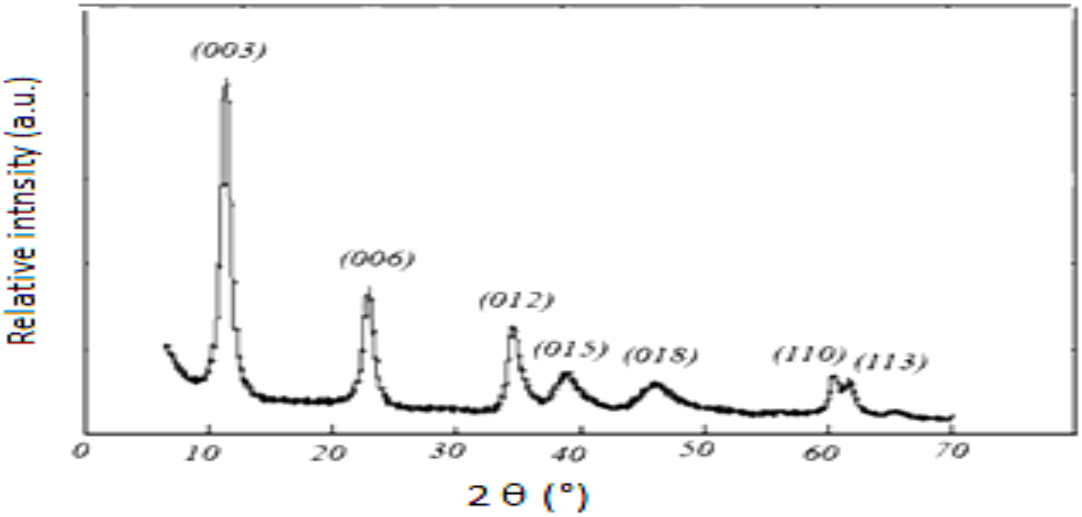

Figure.1. X-ray powder diffraction pattern of HT

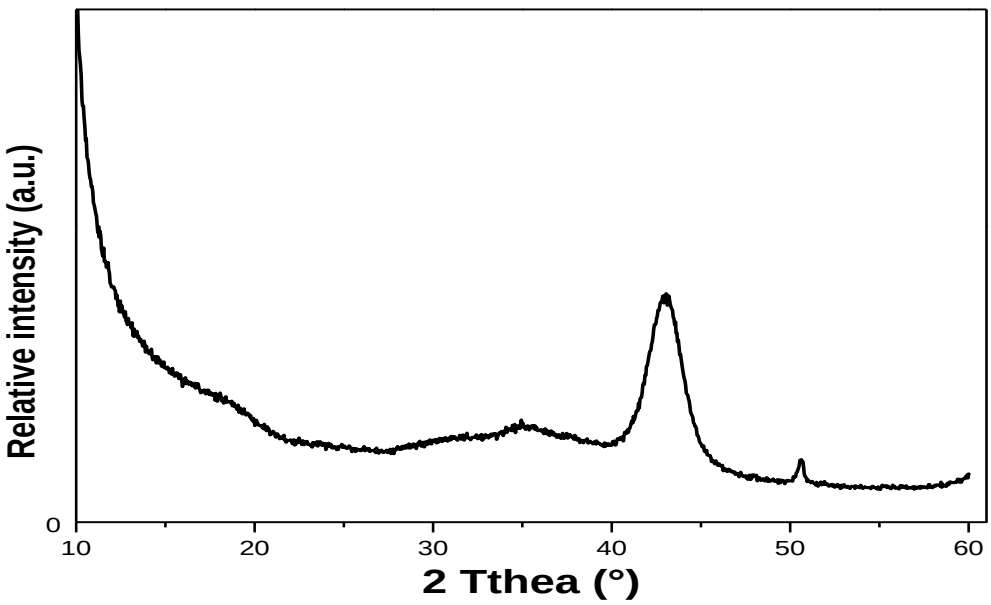

Figure.2. X-ray powder diffraction pattern of HT500

3.1.2 Infrared Spectroscopy

The IR spectra of synthesized anion clays (Figure 3) resemble those of other hydrotalcite like phases [21]:

The band at 3463 $cm^{-1}$is attributed to the stretching vibration of hydroxyl group. The low intensity band at 1637 cm^{-1} is assigned to bending vibration of strongly adsorbed water.

The band at 1381 cm^{-1} is assigned to carbonate vibration (CO_3^{2-}), and the bands at 672 and 436 cm^{-1} are respectively due to M–O and O–M–O related to LDH layer (M is a divalent or trivalent metal).

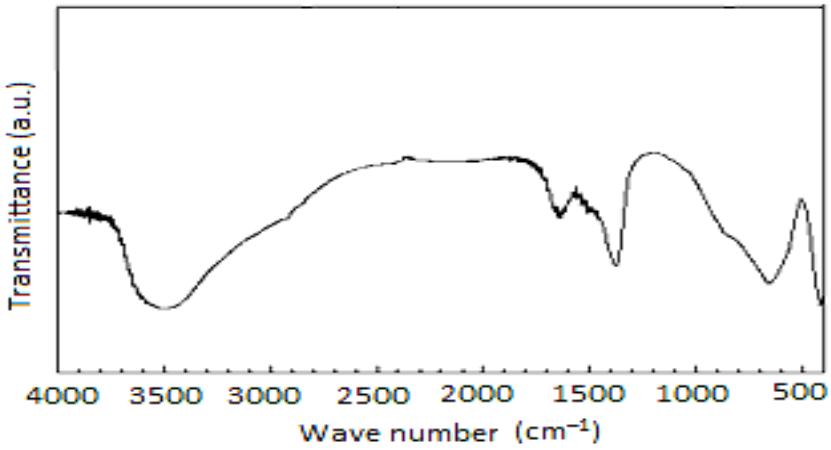

Figure 3. FTIR spectra for HT

3.2Batch adsorption studies

3.2.1 Effect of contact time

The effect of contact time was studied from 10 to 120 min, the initial SO_4^{2-} concentration in effluent is fixed to 480 mg/L. Figure 4 shows that the adsorption of SO_4^{2-} by HT500 is reached quickly in the first stage and then slows considerably as the reaction approache equilibrium. The adsorption equilibrium is reached after 60 min with about 70% of SO_4^{2-} uptake corresponding to 828.29 mg/g as adsorption capacity. Such a rapid uptake is an indication of a high affinity of SO_4^{2-} for the active sites of the HT500 [23]. Limited retention capacity at 70% is due to the presence of other anions such as F^- and HPO_4^{2-}. The same phenomenon is observed when using Nano-alumina as the adsorbent [24].

The adsorption kinetic is analyzed by the pseudo-first-order equation [25], eq. (3) and pseudo-second-order [26-27], eq. (4).

$$\ln(q_e - q_t) = \ln(q_e) - t.K_{1,ads} \quad (3)$$

$$t/q_t = t/q_e + 1/(q_e^2 . K_{2,ads}) \quad (4)$$

Where q_e and q_t (mg/g HT500) are the amounts of SO_4^{2-} adsorbed at equilibrium and at any time t (min), respectively, $K_{1,ads}$ and $K_{2,ads}$,are the rate constants of the pseudo-first-order (figure 5) and pseudo-second-order model (figure 6), respectively. The experimental equilibrium data can be fitted by eq. (3) and (4).The value of R^2 indicates that SO_4^{2} adsorption is successfully fitted by pseudo-second-order model.

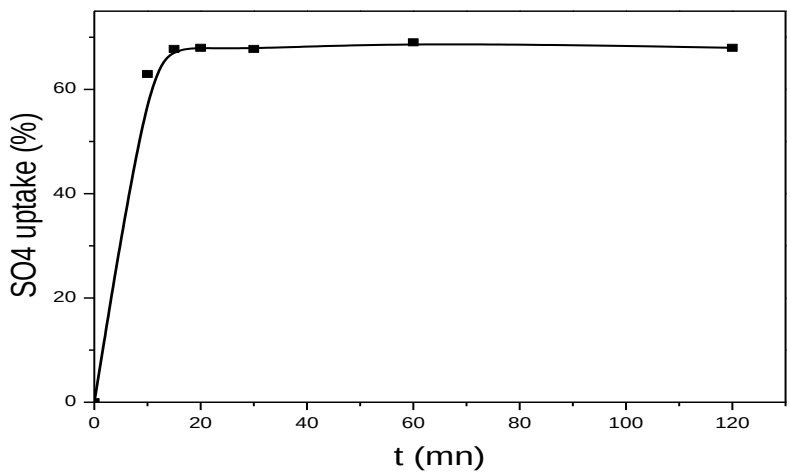

Figure. 4:.Effect of contact time (C_0 = 480mg/L, m_{HT} = 20 mg, T: 25°C, pH=6)

Table.2.Fitting parameters for the SO_4^{2-} adsorption kinetic models

pseudo-first-order Model			pseudo-second-order Model		
$K_{1,ads}$ (min^{-1})	q_e (mg/g)	R^2	$K_{2,ads}$ (g/mg/min)	q_e (mg/g)	R^2
0,0893	438 ,11	0,87	0,0076	819,67	0,99

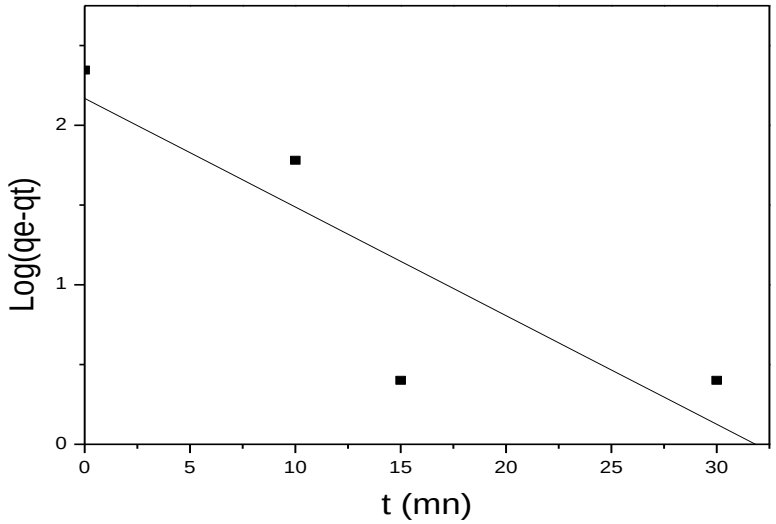

Figure.5. Model of pseudo-first-order for SO_4^{2-} adsorption by HT500

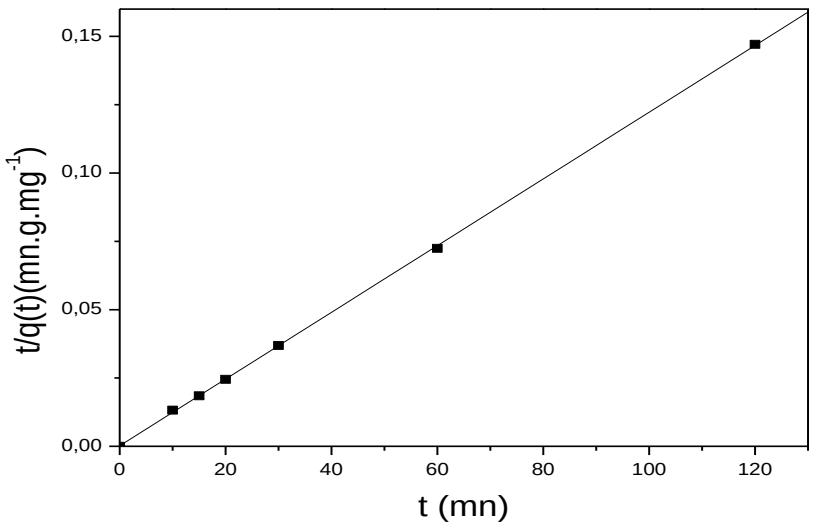

Figure.6. Model of pseudo-second-order for SO_4^{2-}adsorption by HT500

3.2.2. Effect of pH

Generally pH is considered to be an important parameter that controls the adsorption at water adsorbent interfaces. Keeping this in mind, the adsorption of sulfate on HT500 is studied at different pH values ranging from 3 to 8.

The figure 7 shows that the adsorption capacity increases with increasing pH and reached a maximum of 855 mg/gat pH 6.0 before decreasing to 762 mg/g at pH 8. At low pH, the adsorption capacity is low, probably due to the dissolution of layered materials in acid medium. At pH > 6, the decrease of adsorption capacity is due to the competition with OH^-groups for the adsorption sites.

Similar observations have been on the pH dependence of fluoride ions adsorption by Zn-AL-LDH. [28]

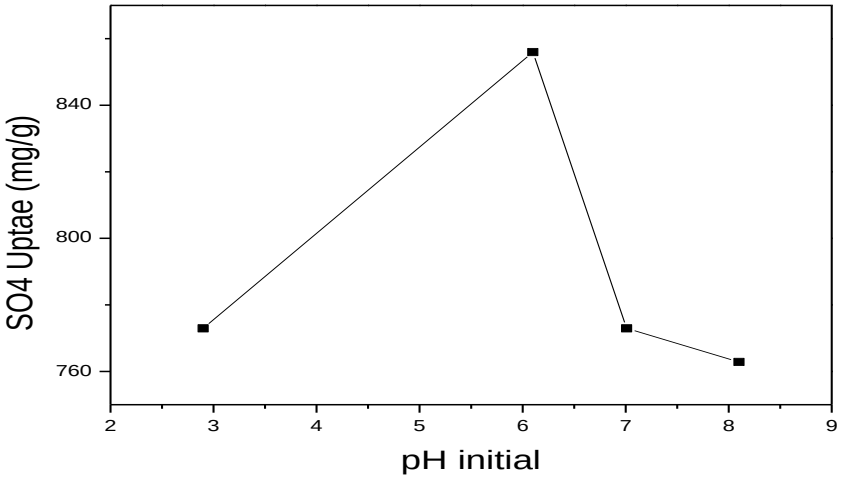

Figure.7. Effect of initial pH (m_{HT500} = 20 mg, C_0 = 480 mg/L, t = 60 mn, T = 25°C)

3.2.3. Effect of adsorbent mass

The effect of adsorbent dose is studied by varying the amount of the adsorbent from 5 mg to 100 mg (Figure 8).

The retention sulfate process by various masses of HT500 is done in two steps. In effect, Figure 8 shows an increase of the retention effluent percentage from 56 to71% when the mass of the adsorbent increases from 5 to 20 mg, this may be explained by the increase of the adsorbent sites, however the level of curve from 20mg to 100mg is due to the saturation of the HT500 sites.

Consequently, the optimal adsorbent mass of HT500 is 20 mg to remove about 71 % of SO_4^{2-}effluent.

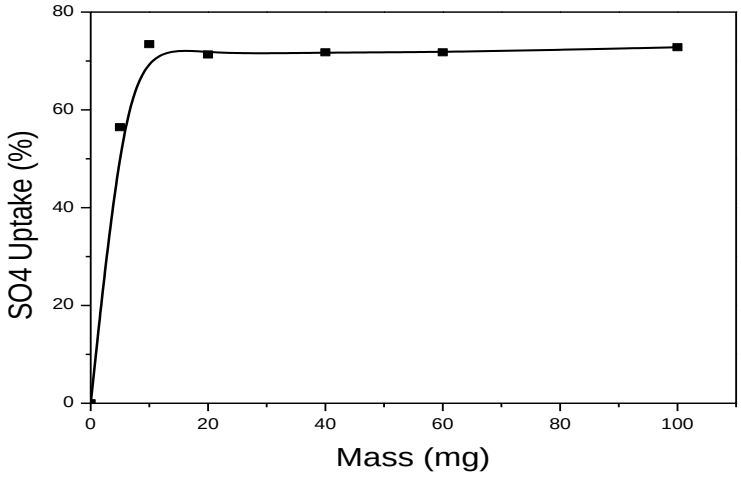

Figure.8. Effect of adsorbent mass (C_0=480 mg/L, pH = 6, T: 25°C)

3.2.4. Effect of initial sulfate concentration

The effect of initial concentration of SO_4^{2-} is studied by varying SO_4^{2-} concentration in effluent from 48 mg/L to 480 mg/L at 298 °K. Adsorbent dose is taken to 0.4g/L (Figure 9).

Figure 9 shows that the removal efficiency increases when the initial sulfate concentration increases from 63,36 % for 48 mg/L to 75,22 % for 240 mg/L, and decreases at 70,91 % for 480 mg/L.

At low initial SO_4^{2-} concentrations, the available sorption sites are easily occupied by SO_4^{2-} resulting in higher removal efficiencies. However, as the initial concentration of SO_4^{2-}increased, most of the available

sorption sites became occupied, leading to a decrease in the removal efficiency. It indicates a decrease in the active sites on the sorbents as more adsorbate are adsorbed.

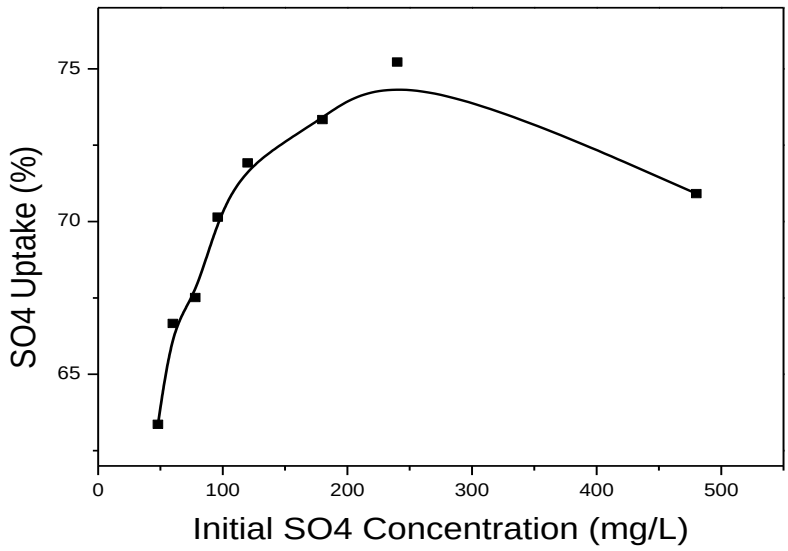

Figure.9. Effect of initial SO_4^{2-} concentration (HT500 dose: 0.4 g/L, T: 25°C, pH 6)

3.2.5. Adsorption isotherm

Figure 10 shows the adsorption isotherm of SO_4^{2-} effluent by HT500. The experimental equilibrium data can be interpreted by Langmuir and Freundlich equations (5) and (6).

$$C_e/q_e = 1/(K_L.q_m) + (1/q_m)C_e \quad (5)$$

$$\ln q_e = \ln (K_F) + (1/n)\ln C_e \quad (6)$$

Where q_e is the amount of SO_4^{2-} adsorbed by HT500 at equilibrium; q_m is the saturated adsorption capacity of the SO_4^{2-} by HT500; K_L, a constant of the Langmuir isotherm and C_e, the equilibrium concentration of the SO_4^{2-} in effluent; K_F and 1/n are the parameters of the Freundlich isotherm.

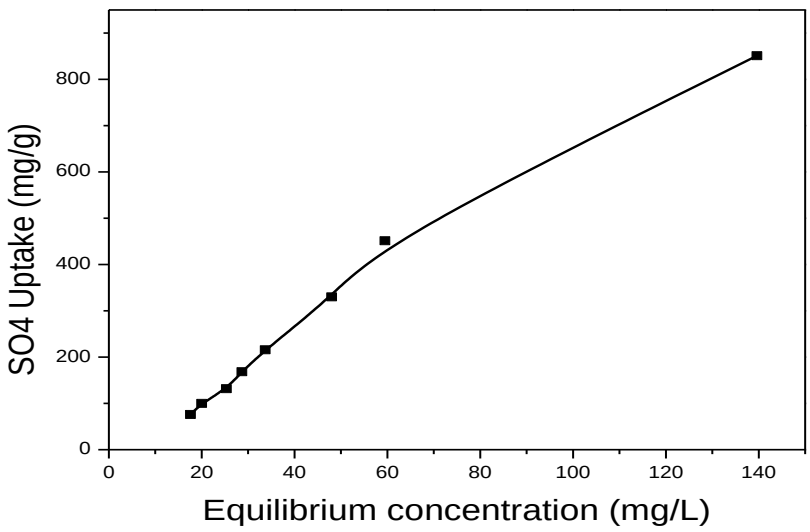

Figure.10. Adsorption isotherm of the SO_4^{2-} on HT500 (HT500 dose: 0.4 g/L, T: 25°C, pH 6)

The experimental equilibrium data can be fitted by the equations (5) and (6).The value of R^2 (~ 0.99 for Freundlich) indicates that SO_4^{2-} adsorption is successfully fitted by the Freundlich isotherm model (Figure 11).

The maximum capacity K_F is 3,81 mg/g $(L/mg)^{1/n}$ and the adsorption constant 1/n is 0.88. The value of 1⁄n between 0 and 1 represents good adsorption of SO_4^{2-} on HT500 [23]. The value of the maximum capacity is close to those reported in literature of adsorption of sulfate by LDH on an aqueous solution [23].

As it's known, the Langmuir model is applicable to homogeneous adsorption where the adsorption of each sorbate molecule onto the surface had equal adsorption activation energy, while the Freundlich model is employed to describe heterogeneous systems and reversible adsorption, which is not restricted to the formation of monolayer. wich explain, the retention rate of sulfate ions which does not exceed 75% because of other anions present in the discharge, especially fluoride (F^-), the nitrate (NO_3^-) that may occupy some sites of the surface.

Thus, the adsorption isotherm of SO_4^{2-} effluent by HT500 reflects a physisorption type between the adsorbate and the adsorbent. This result can be confirmed by the thermodynamic study.

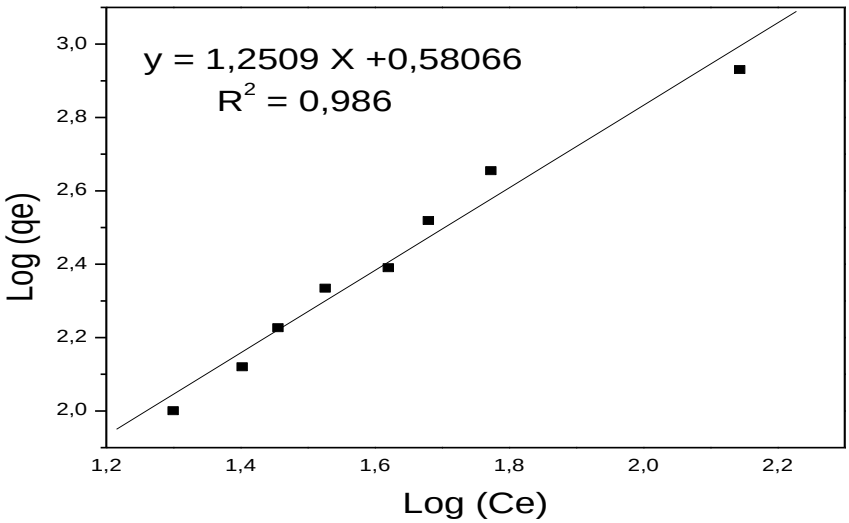

Figure.11. Freundlich isotherm for SO_4^{2-} adsorption by HT500

3.3. Thermodynamic Parameter

Thermodynamic parameters are evaluated by considering the thermodynamic equilibrium constants. The standard free energy is calculated using the following equation:

$$\Delta G^\circ = -RT \ln K \qquad (7)$$

Where ΔG°_{ads} is the free energy change (kJ/mol), T is the absolute temperature (K), R is the universal gas constant (8.314×10^{-3} kJ/K mol), K is the thermodynamic equilibrium constants obtained using the method of Khan and Singh [29].

$$K = a_s/a_e = v_s Q_e / v_e C_e \qquad (8)$$

Where $\mathbf{a}_s$ is the activity of sulfate in solid phase on HT500, a_e is the activity of sulfate effluent in solution at equilibrium, ν_s is the activity coefficient of the adsorbed sulfate effluent and ν_e is the activity coefficient of the sulfate effluent in solution at equilibrium. As the sulfate concentration in the solution decreases and approaches zero, the activity coefficient ν approaches to unity. Equation (8) may be written as follows:

$$\lim_{Ce \to 0} a_s/a_e = Q_e/C_e = K \qquad (9)$$

K can be obtained by plotting a straight line of ln(Qe/Ce) versus (Qe) (Figure 12) and extrapolating Qe to zero. Its intercept gives the values of K.

The other thermodynamic parameters, the change in enthalpy (ΔH°) and entropy (ΔS°) are estimated from the following equation:

$$LnK = \Delta S^{\circ}/R - \Delta H^{\circ}/RT \qquad (10)$$

The values of change in enthalpy (ΔH°) and entropy (ΔS°) are calculated from the slope and intercept of the plot of lnK versus (1/T) (table 3).

The negative values of ΔG° imply that the adsorption of sulfates on HT500 is spontaneous. ΔG° value increased with the temperature, indicating that the adsorption process is favorable at high temperature. Since the value of standard enthalpy change, ΔH°, positive, the process is endothermic; the adsorption is physisorption when the value is$\Delta H^{\circ} < 40$ kJ mol^{-1} according to Alkan et al. [30].Therefore, an increase in the temperature leads to a lower adsorption of sulfate at equilibrium, and physical by nature and involves weak forces of attraction. The positive value of ΔS° suggests that the increased randomness at the solid/solution interface for the removal of SO_4^{2-}in effluent.

Similar results are found for the adsorption of Pb (II) by Mg_2Al-LDH [31] or for the defluoridation of drinking water by calcined MgAl-CO_3 layered double hydroxides [32].

Table.3.Thermodynamic parameters for adsorption of SO_4^{2-} in effluent by HT500

T (°K)	K	R^2	ΔG° (KJ mol^{-1})	ΔH° (KJ mol^{-1})	ΔS°(J $mol^{-1}K^{-1}$)
298	3,6765	0,98	-3,228	8,19	38,77
308	4,4999	0,98	-3,854		
328	4,8649	0,99	-4,317		

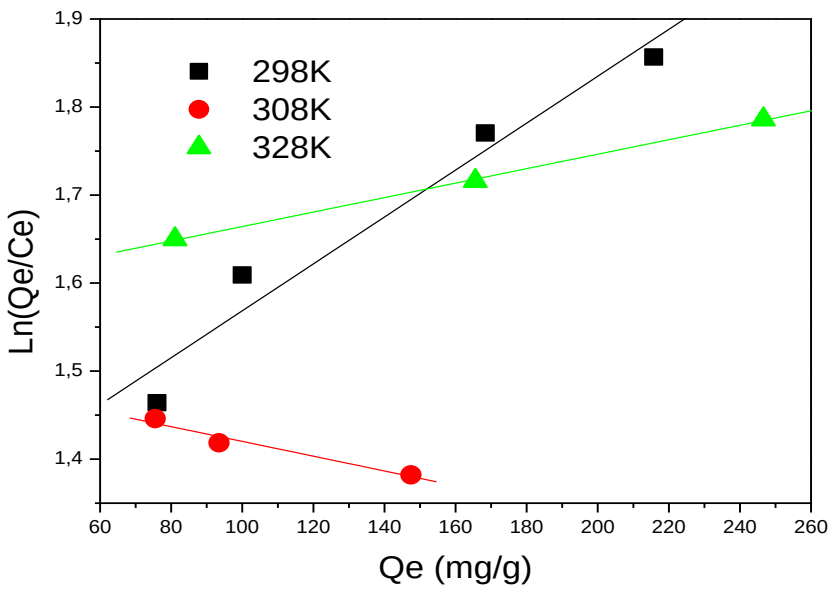

Figure.12. Evolution of ln (Qe /Ce) versus of (Qe).

3.4. Retention mechanism

Calcination of these LDHs produces intermediate non-stoichiometric oxides [18], which undergo rehydration and incorporation of anions in aqueous medium to regain the hydrotalcite structure as expressed by Eqs. (11) and (12) [33]

$$[M^{II}_{1-x}M^{III}_{x}(OH)_2](CO_3)_{x/2} \rightarrow M^{II}_{1-x}M^{III}_{x}O_{1+x/2} + x/2CO_2 + H_2O \qquad (11)$$

$$M^{II}_{1-x}M^{III}_{x}O_{1+x/2} + (x/n)A^{n-} + [1+(x/2)+y]H_2O \rightarrow [M^{II}_{1-x}M^{III}_{x}(OH)_2](A^{n-})_{x/n} + xH_2O \qquad (12)$$

In this study the retention mechanism makes a sulfate anions adsorption at the surface and by intercalation within the regenerated HDL. This result is confirmed by the characterization of the product recuperated after adsorption by XRD. In effect, the X diffractogram obtained (Figure 13) shows the shape type of a LDH. Thus, the interlamellar distance of the order of 8,2026Ǎ is less than that which is obtained in the usually synthesis of $MgAlSO_4$ phase. This can be explained by the preferential orientation of sulfate anion when regenerating HT -SO_4 by the reconstruction method. [34]

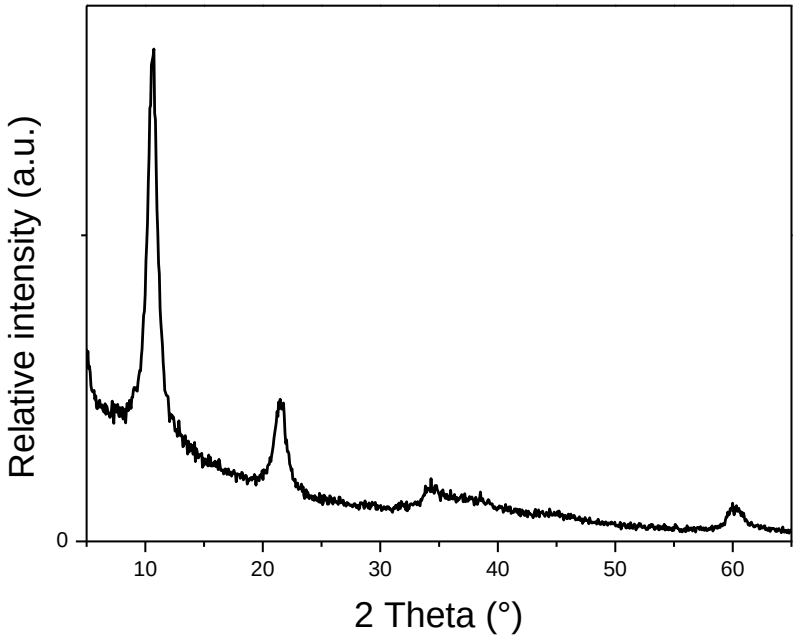

Figure.13. XRD pattern of HT500 after adsorption

Conclusion

The results of the tests conducted during this study allow us to optimize the parameters of adsorption of SO_4^{2-} effluent by HT500 prepared, namely the effect of contact time, pH, adsorbent mass, dose of the adsorbate and temperature.

It'is found that the maximum loading capacity of 828 mg/g is observed at an adsorbent dose of 0.4g/L, sulfate concentration 480 mg/L, pH 6.0 and 60 min equilibrium time. The adsorption kinetics is best described by the pseudo-second-order model, while equilibrium adsorption isotherms are best fitted with Freundlich isotherm equation. The saturated adsorption capacity of HT500 is 3,81 $(mg/g)(L/mg)^{1/n}$.

The thermodynamic study showes that the adsorption is physisorption process ($\Delta H° < 40$ kJ mol^{-1}), spontaneous ($\Delta G° < 0$) and endothermic.

The results of XRD after adsorption, demonstrate that the main adsorption mechanism involves the rehydration of mixed metal oxides and concomitant intercalation of SO_4^{2-} into the interlayer to reconstruct the LDH structure. The above results permit to conclude that calcined hydrotalcite exhibit an interesting adsorption properties removing the sulfate SO_4^{2-} from wastewater effluent.

References

1. Maree J. P., greben H. A., beer. M., *Water SA.* 30(3) (2004) 183-189.
2. Benatti C. T., tavares C. R. G., lenzi. E., *Journal of Environmental Management*. 90(1) (2009) 504-511.
3. Tait S., Clarkeb W. P., keller. J, batstonea. D. J. *Water Research*, 43(3) (2009) 762−772.
4. Basha C. A., Selvi S.J., Ramasamy E., chellammal S., *Chemical Engineering Journal*, 141 (2008) 89-98.

5. Lee h. j., Oh S. J., moon s. h. *Water Research*. (2003).
6. Galiana-Aleixandre M. V., Iborra-Clar A., Bes-Pifi A., Mendoza-Roca J. A., Cuartas-Uribe B., Iborra-Clar. M. I., *Desalination*. 179 (2005) 307-313.
7. Bódalo .A., Gómez .J. L., Gómez .E., León. G., Tejera .M., *Desalination*. 162 (2004) 55-60.
8. Abali M., Ait Ichou .A, Abidar .F., Soudani .A., Sinan .F., Zerbet .M., M. Chiban. *J. Mater. Environ. Sci*. 5 (2014) 2432-2437.
9. Zhang L. Y., Chai L. Y., Wang H. Y., Liu Q., Tan X. B., *Journal of Central South University Science and Technology*. 41 (2010) 422-427.
10. Zhao F., Rahunen N., Varcoe J.R., Chandra A., Rossa C.A., Thumser A. E., Slade R C T., *Environmental Science and Technology*. 42(13) (2008) 4971-4976.
11. Boukhalfa C., *Desalination*. 250 (2010) 428-432.
12. Kolics A., Polkinghorne J. C., Wieckowski A., *Electrochimica Acta*., 43 (1998) 2605-2618.
13. Sag Y., Aktay y., *Process Biochemistry*. 36 (2000) 157−173.
14. Sabbar E., Marie E. R., Fabrice L., *Microporous and mesoporeuxMatereil*. 103 (2007) 134-141.
15. Sabbar E., Marie E. R., Fabrice L. *Journal of Physics and Chemistry of Solids*. 67 (2006) 2419-2429.
16. Sadik N., Sabbar E., Mountadar .M. *Mater. Environ. Sci*. 3 (2012) 379-390.
17. Sadik R., Lahkale R., Hssaine N., Diouri .M., Sabbar E., *IOSR*. 8 (2014).
18. Miyata S., *Clays and Clay Minerals.* 28 (1980) 50-56.
19. Sadik N., Mountadar M., Sabbar E. *J. Mater. Environ. Sci.* 6 (2014) 2239-2246.
20. Reichle WT., *Solid State Ionics*. 22 (1986) 135-141.
21. Lv L., He J., Wei M., Evans D G., Duan X. *Water Research*. 40 (2006) 735-743.
22. Li .Y., Gao .B,. Wu T., Wang B., Li X., *Journal of Hazardous Materials*. 164 (2009) 1098-1104.
23. Halajnia .A., Oustan S., Najafi N., Khataee A.R., Lakzian A., *Applied Clay Science*. 80 (2013) 305-312.
24. Amit B., Eva K., Mika S., *Chemical Engineering Journal.* 163 (2010) 317-323.
25. Lagergren S., *Handl. Bihay.* 24 (1898) 39.
26. Ho Y.S., *PhD Thesis. Birmingham,UK University of Birmingham* (1995).
27. Ho Y.S., Mckay G., T *Water Res*. 34 (2000) 735-742.
28. Mandal S., Mayadevi S., *Applied Clay Science*. 40 (2008) 54-62
29. Khan A.A., Singh R.P., *Colloids Surf. 24 (*1987) 33-42.
30. Alkan M., Demirbas O., Celikcapa S., Dogan M., *Hazard. Mater*. 116 (2004) 135-145.
31. Zhao D., Sheng G., Hu J., Chen C., Wang X., *Chemical Engineering Journal*. 171 (2011) 167-174.
32. Lv L., *Desalination*. 208 (2007) 125-133.
33. Chatelet L., Bottero J.Y., Yvon J., Bouchelaghem, A., *Colloids Surf A*. 111 (1996) 167-175.
34. Susanta P., Jim H.M., *Applied Surface Science.* 263 (2012) 633-639.

(2015); http://www.jmaterenvironsci.com/